AFRL-AFOSR-VA-TR-2024-0054

Influence of Mach number, non-adiabatic walls and nonlinear interactions in resolvent analysis of compressible turbulent boundary layers

Mckeon, Beverley
CALIFORNIA INSTITUTE OF TECHNOLOGY
1200 E CALIFORNIA BLVD
PASADENA, CA, 91125
USA

12/04/2023
Final Technical Report

Air Force Research Laboratory
Air Force Office of Scientific Research
Arlington, Virginia 22203
Air Force Materiel Command

REPORT DOCUMENTATION PAGE

PLEASE DO NOT RETURN YOUR FORM TO THE ABOVE ORGANIZATION.

1. REPORT DATE	2. REPORT TYPE	3. DATES COVERED	
20231204	Final	START DATE 20200622	END DATE 20230621

4. TITLE AND SUBTITLE
Influence of Mach number, non-adiabatic walls and nonlinear interactions in resolvent analysis of compressible turbulent boundary layers

5a. CONTRACT NUMBER	5b. GRANT NUMBER	5c. PROGRAM ELEMENT NUMBER
	FA9550-20-1-0173	61102F
5d. PROJECT NUMBER	**5e. TASK NUMBER**	**5f. WORK UNIT NUMBER**

6. AUTHOR(S)
Beverley Mckeon

7. PERFORMING ORGANIZATION NAME(S) AND ADDRESS(ES)
CALIFORNIA INSTITUTE OF TECHNOLOGY
1200 E CALIFORNIA BLVD
PASADENA, CA 91125
USA

8. PERFORMING ORGANIZATION REPORT NUMBER

9. SPONSORING/MONITORING AGENCY NAME(S) AND ADDRESS(ES)	10. SPONSOR/MONITOR'S ACRONYM(S)	11. SPONSOR/MONITOR'S REPORT NUMBER(S)
Air Force Office of Scientific Research 875 N. Randolph St. Room 3112 Arlington, VA 22203	AFRL/AFOSR RTA1	AFRL-AFOSR-VA-TR-2024-0054

12. DISTRIBUTION/AVAILABILITY STATEMENT
A Distribution Unlimited: PB Public Release

13. SUPPLEMENTARY NOTES

14. ABSTRACT
The challenges associated with observing high-speed boundary layers are well known. In the turbulent regime, there is rarely sufficient observation time to fully characterize statistics or structures. Models for understanding and for large eddy simulation typically rely on a range of assumptions and empirical but tested assumptions. In this work, we seek to develop resolvent analysis for developing turbulent boundary layers under conditions approaching realistic for applications of interest, in particular with regards to Mach number and wall cooling. The subsequent results are used to describe commonalities and differences between the flows of interest and incompressible turbulent boundary layers, with a view to understanding when and how knowledge from the better-studied incompressible case may be applied to compressible turbulence, as well as characterizing the physical forcing exciting truly compressible responses in the flow. We exploit the latter for a proof of concept demonstration of modeling the disturbance field radiated into the freestream from a turbulent boundary layer, an important concern for stability experiments on models mounted in the freestream.

15. SUBJECT TERMS

16. SECURITY CLASSIFICATION OF:			17. LIMITATION OF ABSTRACT	18. NUMBER OF PAGES
a. REPORT	b. ABSTRACT	c. THIS PAGE		
U	U	U	UU	15

19a. NAME OF RESPONSIBLE PERSON	19b. PHONE NUMBER *(Include area code)*
DOUGLAS SMITH	314 235 6013

Standard Form 298 (Rev.5/2020)
Prescribed by ANSI Std. Z39.18

Report Coversheet

Award Number

FA9550-20-1-0173

Report Type

Final

Reporting Period

07/01/2020-06/30/2023

Distribution Statement

Distribution A – Approved For Public Release

Program Officer Name

Dr. Douglas Smith

Principal Investigator Name

Dr. Beverley J. McKeon

Project Title

Influence of Mach number, non-adiabatic walls and nonlinear interactions in resolvent analysis of compressible turbulent boundary layers

ABSTRACT

The challenges associated with observing high-speed boundary layers are well known. In the turbulent regime, there is rarely sufficient observation time to fully characterize statistics or structures. Models for understanding and for large eddy simulation typically rely on a range of assumptions and empirical but tested assumptions. In this work, we seek to develop resolvent analysis for developing turbulent boundary layers under conditions approaching realistic for applications of interest, in particular with regards to Mach number and wall cooling. The subsequent results are used to describe commonalities and differences between the flows of interest and incompressible turbulent boundary layers, with a view to understanding when and how knowledge from the better-studied incompressible case may be applied to compressible turbulence, as well as characterizing the physical forcing exciting truly compressible responses in the flow. We exploit the latter for a proof of concept demonstration of modeling the disturbance field radiated into the freestream from a turbulent boundary layer, an important concern for stability experiments on models mounted in the freestream.

FINAL REPORT

Contract/Grant Title: Influence of Mach number, non-adiabatic walls and nonlinear interactions in resolvent analysis of compressible turbulent boundary layers

Contract/Grant #: FA9550-20-1-0173

Reporting Period: June 2020 to June 2023

Abstract

The challenges associated with observing high-speed boundary layers are well known. In the turbulent regime, there is rarely sufficient observation time to fully characterize statistics or structures. Models for understanding and for large eddy simulation typically rely on a range of assumptions and empirical but tested assumptions. In this work, we seek to develop resolvent analysis for developing turbulent boundary layers under conditions approaching realistic for applications of interest, in particular with regards to Mach number and wall cooling. The subsequent results are used to describe commonalities and differences between the flows of interest and incompressible turbulent boundary layers, with a view to understanding when and how knowledge from the better-studied incompressible case may be applied to compressible turbulence, as well as characterizing the physical forcing exciting truly compressible responses in the flow. We exploit the latter for a proof of concept demonstration of modeling the disturbance field radiated into the freestream from a turbulent boundary layer, an important concern for stability experiments on models mounted in the freestream.

Accomplishments

RESEARCH OBJECTIVES

Extend resolvent analysis to study hypersonic Mach number, non-adiabatic wall, spatially-developing compressible boundary layers, and consider the impact of the modifications of the nonlinear forcing due to compressibility and wall boundary condition.

Specific objectives are outlined as follows:

1. Extend the present quasi-parallel resolvent formulation, which is based on the exceedingly cheap computations associated with a one-dimensional turbulent mean profile, to the spatially-developing case, incorporating state-of-the-art techniques to exploit the low-rank nature of the resolvent operators associated with a two-dimensional mean field.

2. Investigate resolvent model representations of such hypersonic turbulent boundary layers, i.e. determine the weights on the linear resolvent modes to optimally reconstruct the flow-field.

3. Extend the previous investigation to incorporate higher Mach numbers, where effects of compressibility identified in our earlier study are expected to dominate essentially incompressible physics.

4. Consider the influence of a non-adiabatic wall boundary condition on the analysis. It is known that the mean velocity for a non-adiabatic wall does not collapse with semi-local scaling, so some deviation from incompressible and adiabatic wall results (which have been shown to collapse well where acoustic modes are not important) are expected in the analysis. Preliminary results showed this to be the case, but a detailed study which characterizes the differences and the wavenumber regimes where they occur was required.

5. Investigate both the form of the resolvent forcing modes (available from the linear analysis) and the forcing obtained from nonlinear interaction of resolvent modes (which differs from the incompressible case because of the fluctuations in density and temperature) in order to identify similarities and differences associated with the introduction of the thermodynamic variables, and the importance of acoustic modes in turbulent boundary layers.

6. Construct a low-order model of the compressible TBL, exploiting the developments from each of the other objectives. The fluctuations and stresses derived from self-interaction of modes feed back to the mean fields, providing a means to support the input mean fields, effectively as constraint on nonlinear low-order models.

ACCOMPLISHMENTS DURING REPORTING PERIOD

Work has been completed on objectives 1-5 and for a specific configuration under objective 6. Here we provide a brief summary of activities throughout the award period. More details are given in the Technical Update section. The work has led to the following accomplishments:

- Implementation of local and biglobal resolvent analyses to examine spatially-developing, high-speed turbulent boundary layer flows.
- Characterization of the response of a supersonic flow with an adiabatic wall to stochastic forcing.
- Characterization of the response of supersonic and hypersonic boundary layers with adiabatic walls to deterministic forcing.
- Distillation of the key variations with increasing Mach number and with wall cooling for local resolvent analysis, i.e. under a quasi-static approximation and considering a one-dimensional mean profile and for the biglobal case.
- Identification and verification of the effects of dilatation on compressible wall turbulence.
- Implementation of a Helmholtz decomposition of the **forcing** in the resolvent framework. While other authors have considered this decomposition on DNS fields (the response in our approach), the forcing is shown to have a clean decomposition into effects common with incompressible flows and those associated only with compressible ones.

- Leveraging of the forcing decomposition to model the disturbance field radiating to the freestream and comparison with DNS results. Significant results include the connection between waves radiating from the turbulent boundary layer into the freestream with the inviscid Mack waves that are well known in laminar flow; the isolation of Mach waves via masked resolvent analysis; identification of the source of Mack waves in terms of the forcing exciting them via the equations of motion; connection between the observations of wave angle and resolvent predictions.
- Differentiation between cases where a 2D, biglobal analysis is required from those where the cheaper 1D case suffices. Where do 2D effects become important, and how can they be efficiently modeled within the objectives laid out in the proposal?
- Application of the resolvent methods to modeling radiation from the boundary layer to the freestream, i.e. to connect the freestream disturbance field affecting modeling testing to the tunnel wall boundary layer characteristics.

DISSEMINATION

Work pertaining to this grant has been presented annually at the 2021 and 2022 APS Division of Fluid Dynamics Annual Meetings (and will be in the upcoming 2023 Meeting) and the AIAA SciTech 2022 meeting. We anticipate a submission to the 2024 AIAA Aviation meeting pertaining to work under this funding.

Impacts

The major impact of the work under this grant has been to elucidate differences and commonalities between incompressible and compressible wall turbulence, channels and zero pressure gradient boundary layers in particular, and the effects of Mach number and wall cooling on that analysis using resolvent-based techniques. We have exploited self-similarity of the mean profile as a way to understand self-similarity of turbulent response to forcing, and the Helmholtz decomposition to separate forcing mechanisms that are common across Mach number from those specific to supersonic and hypersonic Mach numbers, and the associated physical structures corresponding to the latter.

This novel interpretation of the nonlinear forcing and linear response in wall turbulence has the potential to permit separate modeling of both types of effect, including for the more practical cooled wall cases as well as adiabatic walls. In separate work, we are investigating how to exploit general resolvent findings to improve the fidelity of low-order and computational models in incompressible flows. This work could naturally be extended to the high-speed regime.

A key aspect of the work is the ability to address the modeling of the Mach wave radiation from the boundary layer into the freestream for hypersonic flows, a question with direct implications for experimental test facilities, and which we have been continuing to investigate as the grant concludes.

In terms of personnel, the graduate research assistant (Stroot) primarily working on the grant has passed his thesis candidacy exam and is thus on track to complete a Ph.D. in approximately the next 12

months in the area of low-order modelling of hypersonic, turbulent wall flows. A second graduate student (Gomez) contributing to the research recently successfully defended his Ph.D. thesis and will continue as a postdoctoral fellow at Stanford University, effective November 2023. The postdoctoral scholar (Madhusudanan) who began the work on this project completed a Simons Fellowship at the University of Cambridge and is now a DST-INSPIRE Faculty Fellow at the Indian Institute of Science.

Changes

There are no changes to report.

Technical Updates – Final Report

We augment the description of Accomplishments above with technical details concerning each of the objectives.

1. Resolvent analysis for spatially-developing boundary layers

We develop resolvent analysis for 1D mean fields (local or 1D analysis), and extend the effort to 2D or biglobal resolvent analysis, which takes specific account of the effects of streamwise development of the boundary layer. Further, we consider masked analyses, in which the response may be restricted to the freestream, i.e. outside of the boundary layer (Figure 1). Full details of the approach may be found in Bae, Dawson & McKeon (2020) and Madhusudanan & McKeon (2022). Notably, we employ the Chu norm for the analysis.

Figure 1: Local and biglobal resolvent analyses, showing masking for the biglobal case in which response is restricted to the freestream.

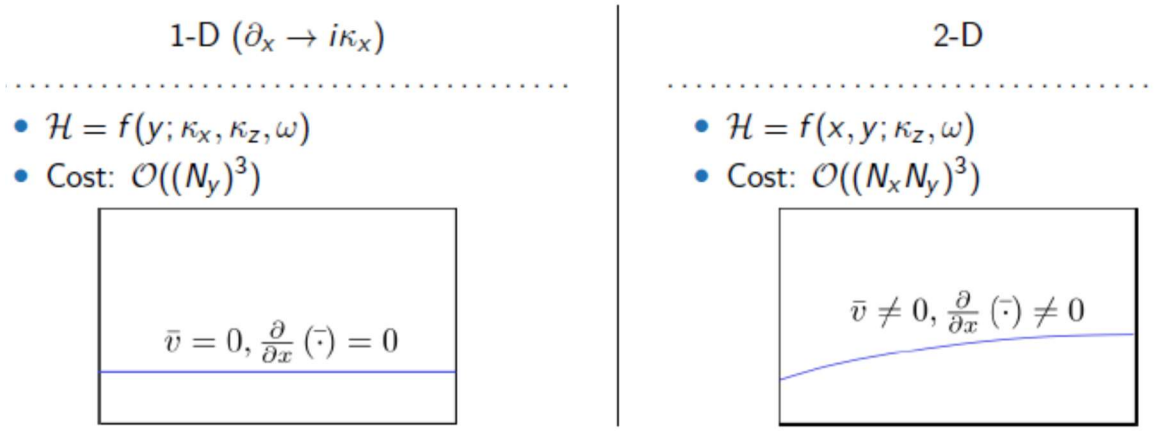

Figure 2: Comparison of local and biglobal resolvent analysis domains and costs.

We consider explicitly the cost of the biglobal vs. the local analysis, as shown in Figure 2, in order to determine when the biglobal response may be estimated in terms of the much cheaper, constrained local response.

2. Resolvent response for hypersonic boundary layers (stochastic forcing)

We began work on this grant by considering the stochastically-forced resolvent (which gives insight into the globally most amplified structures by exciting all possible responses). A sample result over a range of Mach number, Ma, for an adiabatic wall laminar boundary layer, where the analytical base profile allowed us to calibrate our approach and the numerics. Figure 3 shows the resolvent norm in the streamwise/spanwise, (k_x,k_z) plane (results are integrated over wavespeed) for Mach numbers in the range 6-10. Forcing is applied to all variables and the footprint of streaks, elongated regions of coherence for low k_x can be seen in all variables across the Ma range. When the forcing is restricted to the velocity components only, i.e. the density and temperature forcing is removed (Figure 4), the appearance of streaks remains. This motivated a more detailed investigation of the action of the forcing terms. Further, the influence of wall cooling was investigated on the resolvent response.

3. Resolvent response for hypersonic boundary layers (deterministic)

The stochastic response gave some indication of the importance of isolating the forcing via the Helmholtz decomposition into solenoidal and dilatational components and the separate treatment of velocity and thermodynamic responses. We moved on to explicitly consider these for the case with deterministic forcing under the quasi-parallel assumption.

Considering next the deterministic forcing of the resolvent on a mode-by-mode basis, (k_x, k_z, c), where c is the wavespeed, we examined decompositions to isolate the parameter ranges where the response is dominated by velocity vs. density and temperature. The same naïve restriction to velocity forcing did not lead to a separation of the responses (Figure 5, top row), while a very clean separation is obtained by decomposing the forcing into solenoidal and dilatational components given by the singular value decomposition of the resolvent (Figure 5, bottom row). The separation of the two different responses in (k_z,c) space for a given $k_x$is clearly associated with the relative sonic line, demarked by the dashed black line. For long spanwise wavelengths, the response is isolated to be driven by the dilatational forcing, f_d. Streamwise elongated streaks are dominantly driven by the solenoidal forcing, with an increasingly important response associated with the dilational forcing as Ma increases (Figure 6).

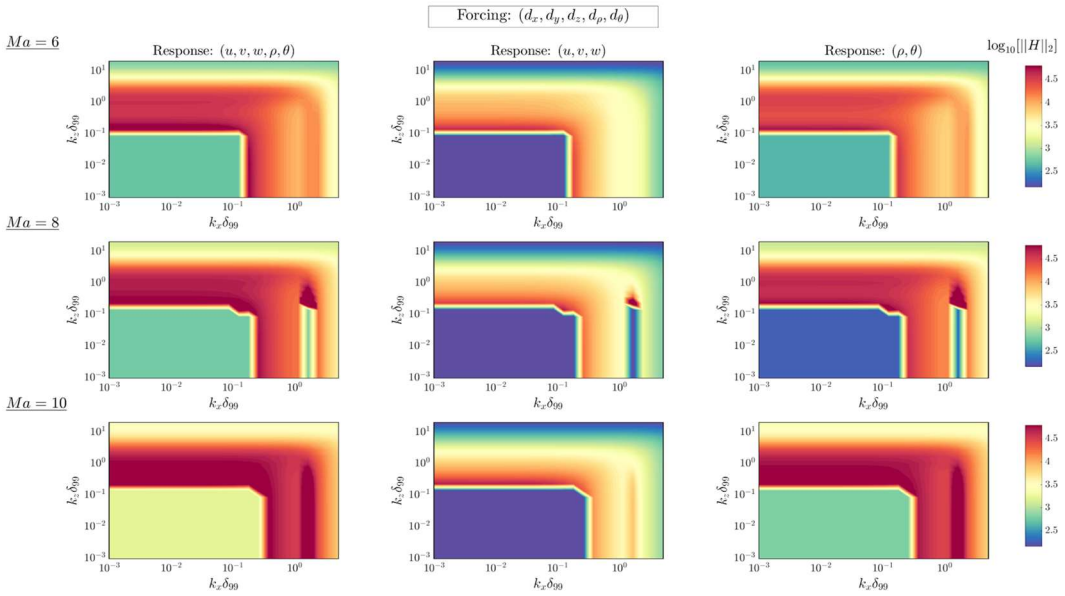

Figure 3: For fixed streamwise wavenumber, Ma=6, Re=300, magnitude of the first singular value of the resolvent. (Stochastic) forcing is applied to all variable and response is separated out into velocity components and density/temperature.

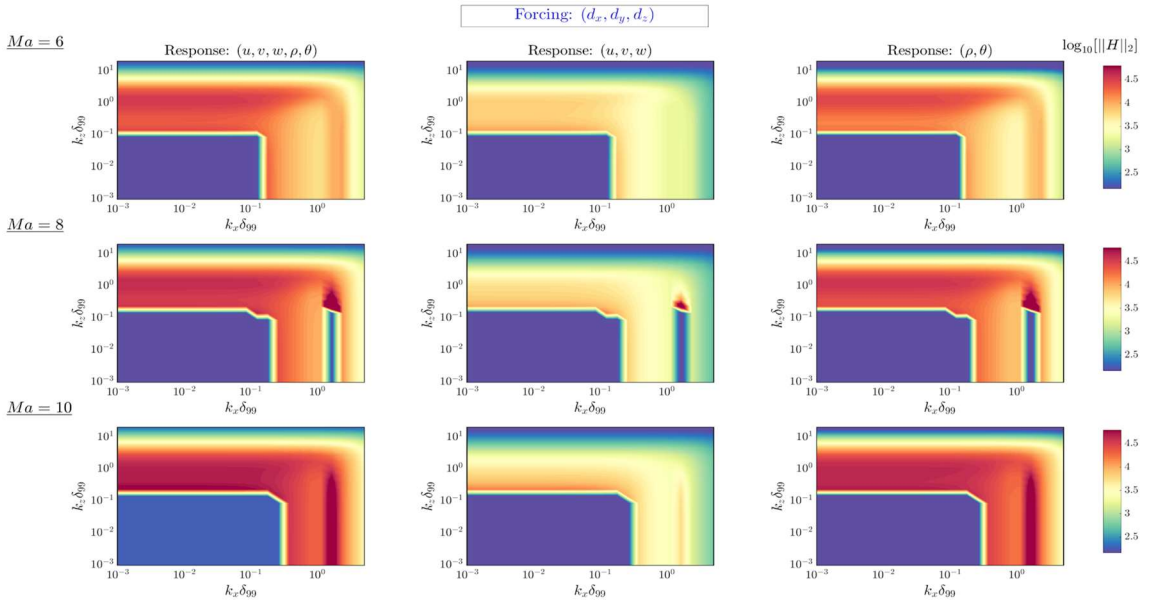

Figure 4: As in Figure 1, but with (stochastic) forcing restricted to the velocity variables only. The footprint of streaks (low streamwise wavenumber) remains in the density and temperature response.

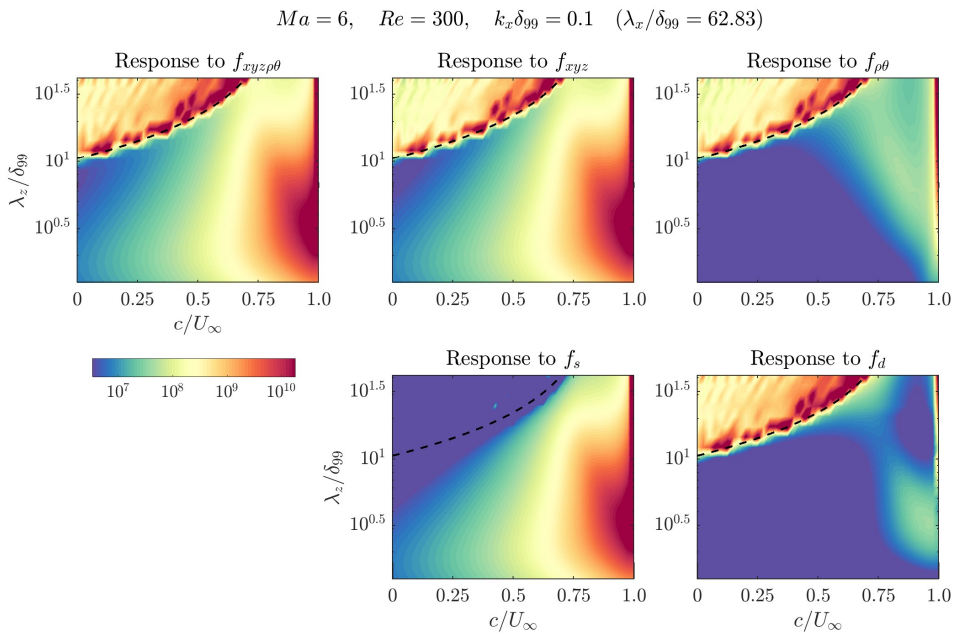

Figure 5: For fixed streamwise wavenumber, Ma=6, Re=300, magnitude of the first singular value of the resolvent for a sweep across spanwise wavenumber and wavespeed. Clockwise, from top left: response to full forcing, response to forcing in the three velocity components only, response to forcing in the density and temperature only, response to dilatational forcing, f_d, and response to solenoidal forcing, f_s

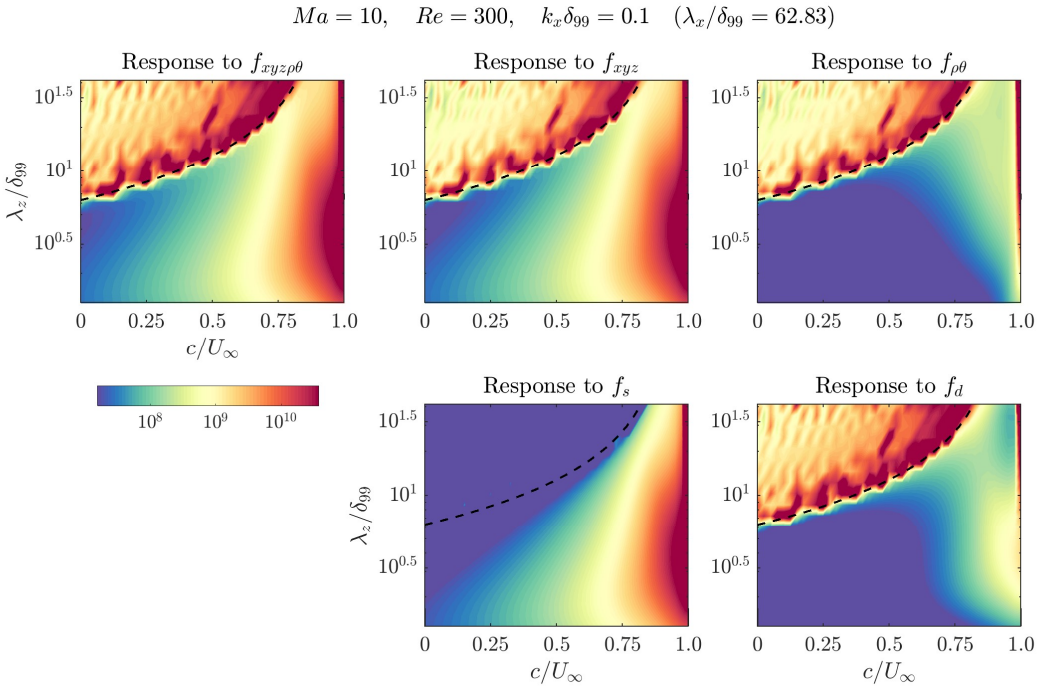

.

Figure 6: As in Figure 5, but for Ma=10.

The importance of the relative sonic speed, demarking disturbances with wavespeeds that are relatively subsonic from those moving supersonically relative to the freestream, had been identified in our previous work (Bae et al). Under this grant, we showed that the subsonic disturbances can be considered to be identical across Mach range for canonical flow configurations with similar mean profiles, i.e. under a semi-local scaling such as that due to Trettel & Larsson for the compressible case.. Figure 7 shows the integrated response (resolvent norm, σ_1) for M=0 and M=4 cases, with the same gray line identifying an isocontour associated from the M=0 case and the diagonal dashed line the relative sonic condition.

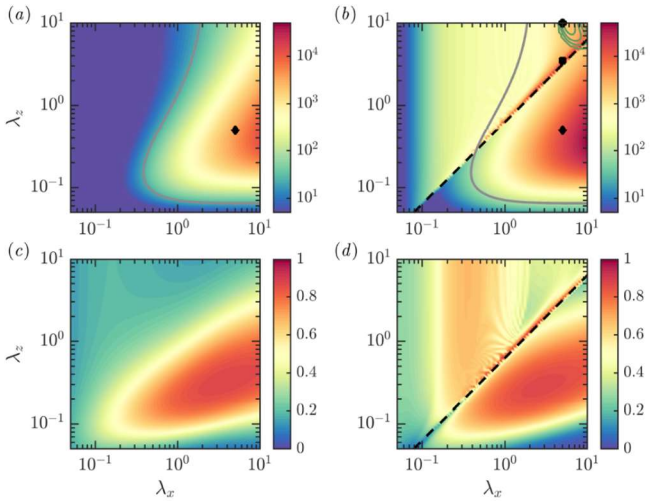

Figure 7: (a,b) The leading resolvent gain σ_1 as well as (c,d) the fraction of energy captured by the leading resolvent mode LR=$\sigma_1^2/(\Sigma_i \sigma_i^2)$, are shown as a function of the streamwise and spanwise wavelengths (lx, lz) and a fixed phase speed c corresponding to $U^+(y^+=15)$. (a,c) An incompressible boundary layer with Re_τ= 450 and (b,d) a compressible boundary layer with Ma=4 and Re_τ = 400 over an adiabatic wall are considered. The black dashed line in (b,d) indicates the relative Mach number equal to unity. The green contours at the top right-hand corner for the compressible case indicates the region of the wavenumber space that is unstable. The grey contour line in (a) indicates 1/3rd of the maximum energy in the incompressible case, and the same contour (computed from the incompressible case) also appears in (b) for comparison. The black symbols indicate the modes that are discussed in later figures.

Figure 8 shows the kinetic energies of the rank-1 approximation of the resolvent, i.e. associated with spatially-integrated ψ_1 for a subsonic mode, including the full response and the separated solenoidal and dilatational components. The separation is relatively clean, however the picture is even clearer when we apply the Helmholtz decomposition to the forcing, ϕ_1 , rather than the response, ψ_1 .

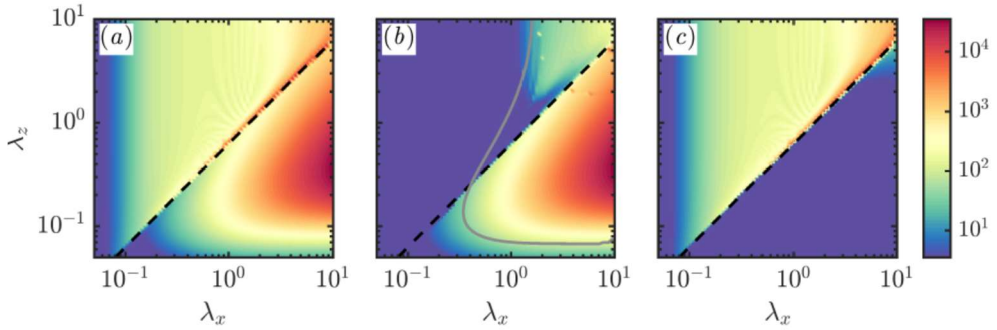

Figure 8: The kinetic energy of (a) the leading resolvent response ψ_1 and of (b) the solenoidal and (c) the dilatational component of the velocity from ψ_1 is shown as a function of the streamwise and spanwise wavelengths and a fixed phase speed c = U⁺(y⁺=15). Ma=4 and Re_τ = 400 over an adiabatic wall.

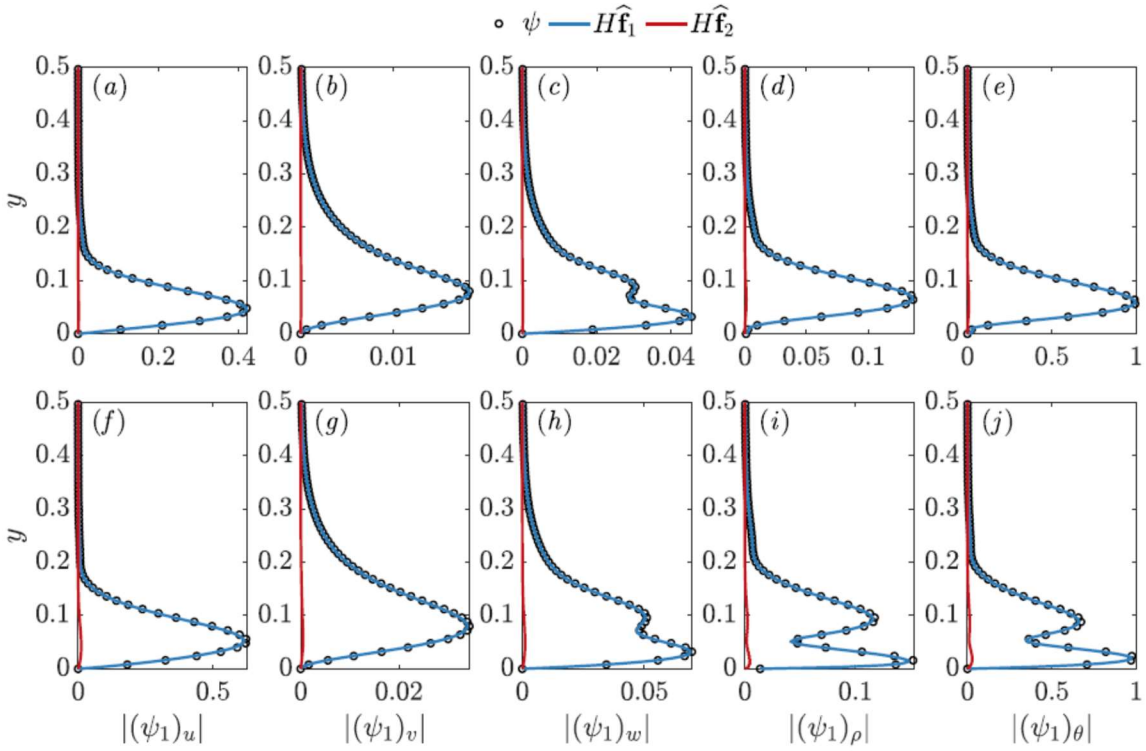

Figure 9: The response of the resolvent operator to the full leading resolvent forcing mode (black) as well as the response to the two components of the forcing: solenoidal (blue) and dilatational (red) are shown. Subsonic modes for two compressible boundary layers are shown: (a-e) Ma=4 and Re_τ = 400 over an adiabatic wall and (f-j) Ma=6, Re_τ=450 with θ_w/θ_{ad}=0.25. The (a,f) streamwise, (b,g) wall-normal and (c,h) spanwise velocities as well as the (d,}) density and (e,j) temperature are shown.

Figure 9 shows that the entirety of the subsonic mode response is captured by the solenoidal part of the forcing (Mach 4 and 6 flows with adiabatic and cooled walls, respectively, shown).

For supersonic modes, we make two observations. First, the response in the freestream is restricted to supersonic modes (not shown), as would be expected. Second, the supersonic modes are forced in the most part by the dilatational forcing, with a small solenoidal part that can be easily identified via the

equation governing the pressure fluctuations. An example mode in support of this result is shown in Figure 10.

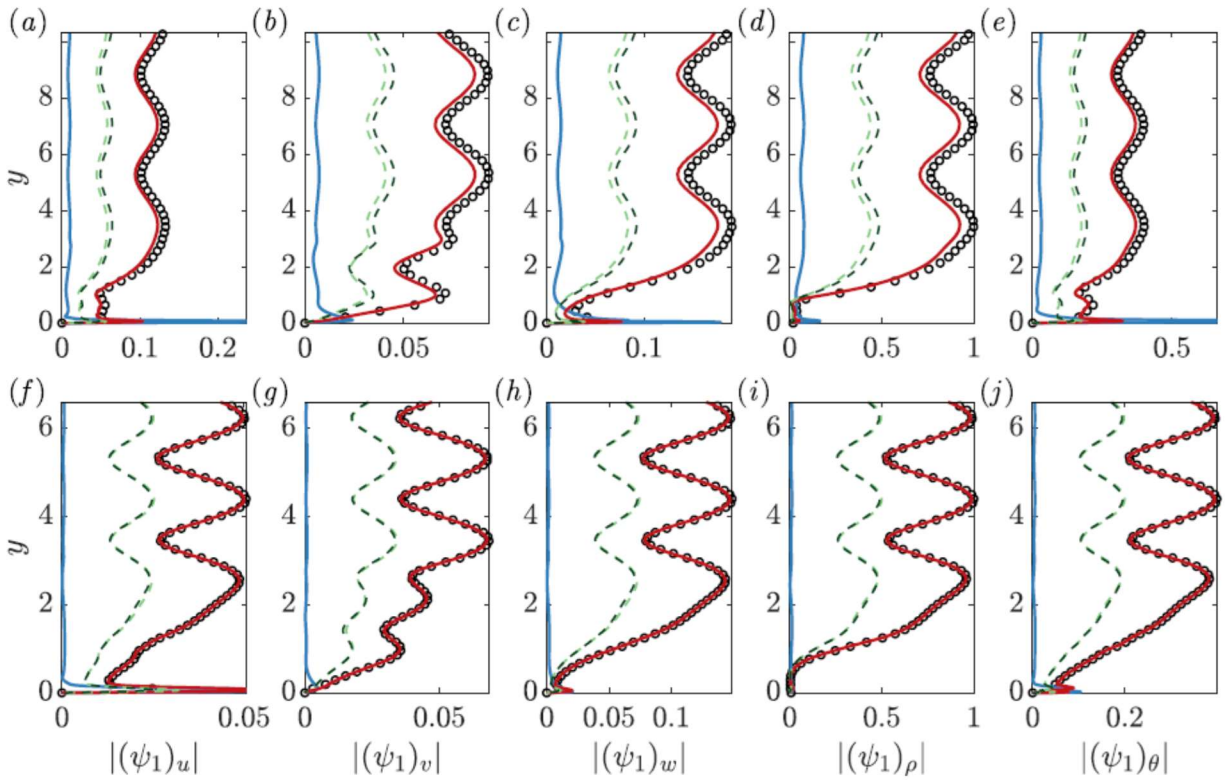

Figure 10: The response of the resolvent operator to the full leading resolvent forcing mode (black) as well as the response to the two components of the forcing: solenoidal (blue) and dilatational (red) are shown. The two green responses are to the thermodynamic and velocity contribution to the dilatational forcing. Supersonic modes that fall close to the relative Mach equal to unity lines are shown for two compressible boundary layers: (a-e) Ma=4 and Re_τ = 400 over an adiabatic wall and (f-j) Ma=6, Re_τ=450 with θ_w/θ_{ad}=0.25. Modes that fall close to the relative Mach equal to unity lines are shown. The (a,f) streamwise, (b,g) wall-normal and (c,h) spanwise velocities as well as the (d,}) density and (e,j) temperature are shown.

Importantly for what follows, the freestream region of the pressure, i.e. the radiation to the freestream, is well-described by the well-known inviscid Mack relationship (Figure 11) developed for instability studies, which can be exploited for modeling purposes.

An analytical relationship for the inclination to the wall of the radiating pressure wave can be determined in terms of the aspect ratio and the phase speed of the mode (Figure 12). The range of angles spans those determined to be the statistically dominant ones in DNS of flows under a range of conditions; the actual prediction from the resolvent model depends on the nonlinear forcing induced in the flow.

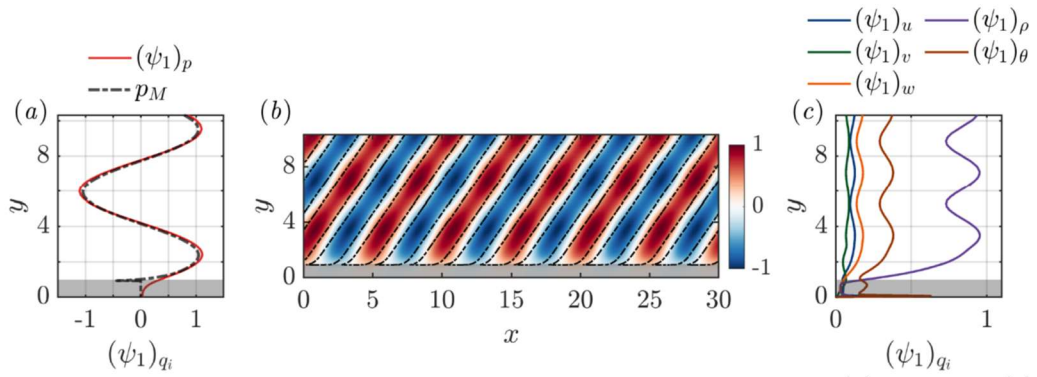

Figure 11: The leading resolvent response for a sample supersonic mode at Ma=4 and Re_τ= 400 over an adiabatic wall. (a) The wall-normal profile of the real part of the pressure from the resolvent mode (red) is compared with the pressure fluctuations from the inviscid Mack wave (black dashed). (b) The pressure fluctuations in a x-y plane is also shown with red (positive) and blue (negative) contours showing the real part of the pressure fluctuation from the resolvent mode and the black contour lines indicating the pressure fluctuations from the inviscid Mach wave at +/- 0.5 of the maximum. (c) The wall-normal profile of the other response components. The grey shaded regions indicate the boundary layer thickness.

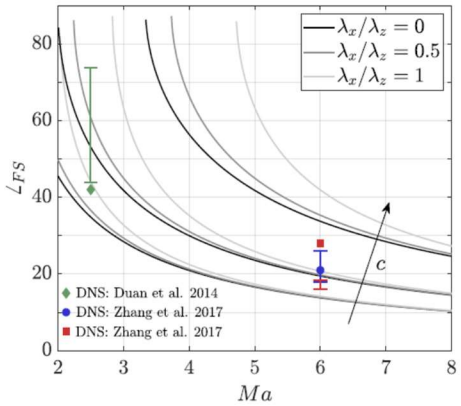

Figure 12: The inclination angle of the radiating Mach waves is shown with respect to Mach number for a range of aspect ratios and phase speeds. Three different phase-speeds of c=0.3,0.5 and 0.7 increasing in the direction of the arrow and three different values of aspect ratios λ_x/λ_z = 0,0.5 and 1.0 are shown. The markers indicate the average inclination angles of the Mach waves from DNS reported in the literature by Duan et al. The DNS data at Ma=6 is for the case of cooled walls, and the two markers indicate two different ratios of θ_w/θ_{ad}=0.76 (blue) and 0.25 (red). The intervals represent the range of inclination angles predicted by the resolvent model under two assumptions: (1) k_z=0 and (2) $U^+(y^+ = 10) < c < U^+(y^+ = 10)$.

4. Towards a low order model of radiated disturbances from hypersonic turbulent boundary layers

In the final piece of the project, we exploited the findings concerning disturbances radiated from the high-speed turbulent boundary layer to make steps towards a computationally efficient and low-order model connecting the freestream statistics to the state of the boundary layer.

First, we explored the relationship between the local and biglobal results for equivalent Reynolds numbers. For the local analysis in a self-similar laminar boundary layer, shown in Figure 13, maximum

amplification is associated with a relatively sonic wavespeed and modes normal to the wall, i.e. with inclination angle of 90°.

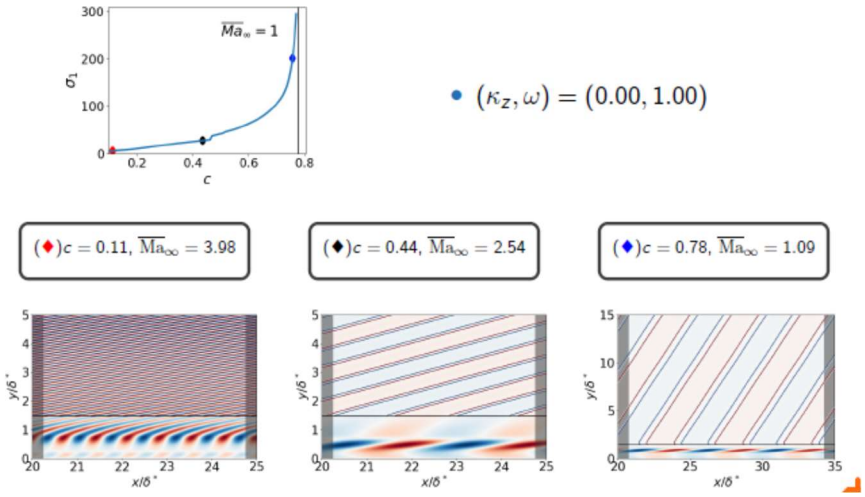

Figure 13: Variation of σ_1 with wavespeed for a given supersonic mode in a (quasi-parallel) turbulent boundary layer. Ma = 4.5 and adiabatic wall. The local resolvent is low-rank; first resolvent modes shown.

The biglobal resolvent for similar parameters is not as low rank, as shown in Figure 14. Here the singular values roll off relatively slowly going down the singular value expansion, with higher modes reflecting beaming (modulation in the streamwise direction). Notably, the maximum amplification occurs for an inclination angle limited by the Mach angle for the flow under consideration.

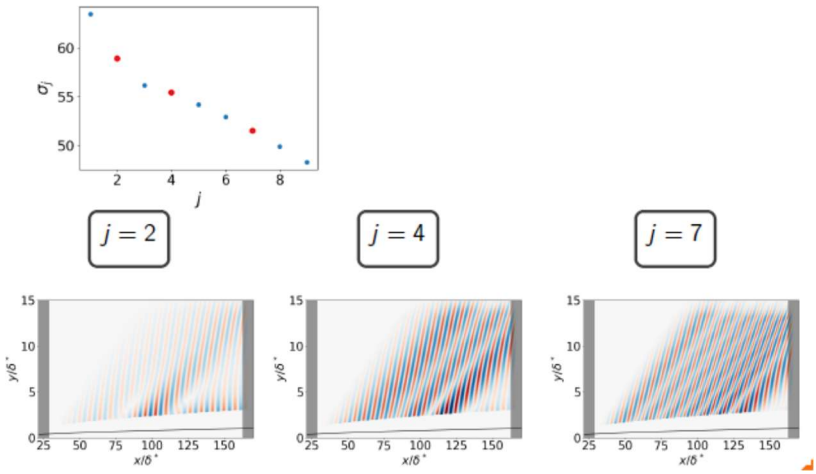

Figure 14: For the same conditions as in Figure 13, but for the biglobal resolvent: radiating structure as a function of position in the singular value decomposition, j.

Nonetheless, the biglobal results can be modeled effectively using local results, the Mach angle restriction and a Gaussian beam envelope (Figure 15).

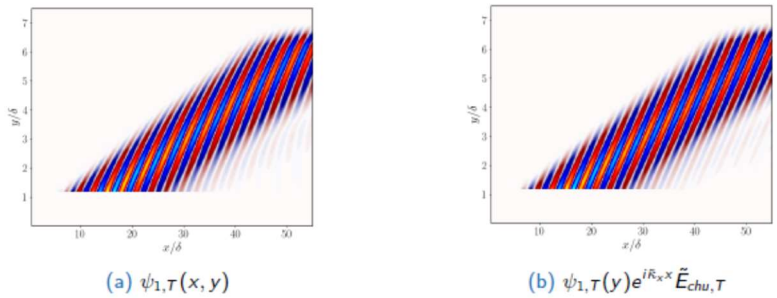

Figure 15: Comparison of the local reconstruction of a given beaming wave (left) and the biglobal results (right) shows reasonable agreement.

Finally, we used local resolvent modes to reconstruct the freestream statistics plotted in Liu et al in their simulation of Ma=8.0 freestream flow above a single wall with a turbulent boundary layer. Just as those authors used a Fourier basis to model the statistics, we used resolvent modes. The origin of these modes can be traced via wavespeed and understanding of relative supersonic mode behavior described above to the region of the boundary layer responsible for the disturbance field. Figure 16 shows the transfer function relationship describing this process and the origin of the disturbances in the buffer layer of the boundary layer, consistent with observations from the DNS of Liu. Inverting this relationship to obtain a predictive model for the freestream disturbance field associated with a given turbulent boundary layer on a tunnel well, is reserved for future work.

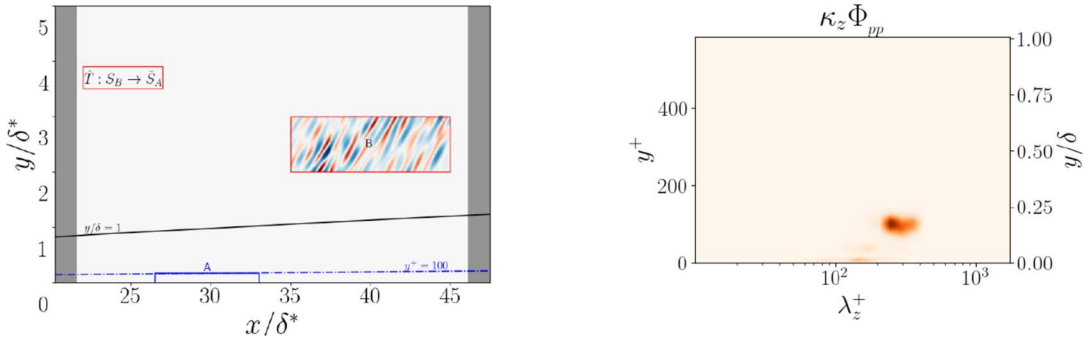

Figure 16: (Left) Schematic showing the transfer function of interest between known freestream disturbance statistics (B) and the state of the boundary layer (A). (Right) spectral representation of the location in the boundary layer of the disturbances that reconstruct the freestream disturbances.

5. Summary

Under this grant, we have performed a fundamental investigation into amplification processes in high speed turbulent boundary layers. By comparison with incompressible wall turbulence at comparable Reynolds numbers, we isolated the Helmholtz decomposition of the nonlinear forcing to the resolvent as an efficient way to separate the driving mechanisms for relatively subsonic and supersonic modes and to provide an effective basis for modeling of the disturbance field radiating to the freestream.

References

Bae, H.J., Dawson, S. & McKeon, B.J. “Resolvent-based study of compressibility effects on supersonic turbulent boundary layers” J. Fluid Mech. 883, A29 (2020).

Chu, B.-T. “On the energy transfer to small disturbances in fluid flow (Part i)”. Acta Mech., 1(3), 215.

Duan, L, Beekman, I. & Martin, M. P. “Direct numerical simulation of hypersonic turbulent boundary layers. Part 3: Effect of Mach number.” J. Fluid Mech., 672, 245 (2011)

Liu, Y., Schabb, M., Duan, L., Paredes, P. & Choudhari, M. “Interaction of a tunnel-like acoustic disturbance field with a blunt cone boundary layer” https://arc.aiaa.org/doi/abs/10.2514/6.2022-3250 (2022)

Di Renzo, M., Williams, C., Urzay, J. & Pirozzoli, S. “Stagnation enthalpy effect on turbulent compression corner flow at Ma=5” Proc. CTR Summer Program (2022)

Madhusudanan, A. & McKeon, B. J. “A resolvent-based perspective on the generation of Mach wave radiation from compressible boundary layers” (arXiv and under review)

Madhusudanan, M. & **McKeon, B. J.** ‘Stochastic forcing to a linearized Navier-Stokes based model for laminar compressible boundary layers’ *AIAA-2022-1370.*

Trettel & Larsson, J. “Mean velocity scaling for compressible wall turbulence with heat transfer” Phys. Fluids, 28 (2) 026102 (2016)

Report Coversheet

Award Number

FA9550-20-1-0173

Report Type

Final

Reporting Period

07/01/2020-06/30/2023

Distribution Statement

Distribution A – Approved For Public Release

Program Officer Name

Dr. Douglas Smith

Principal Investigator Name

Dr. Beverley J. McKeon

Project Title

Influence of Mach number, non-adiabatic walls and nonlinear interactions in resolvent analysis of compressible turbulent boundary layers

ABSTRACT

The challenges associated with observing high-speed boundary layers are well known. In the turbulent regime, there is rarely sufficient observation time to fully characterize statistics or structures. Models for understanding and for large eddy simulation typically rely on a range of assumptions and empirical but tested assumptions. In this work, we seek to develop resolvent analysis for developing turbulent boundary layers under conditions approaching realistic for applications of interest, in particular with regards to Mach number and wall cooling. The subsequent results are used to describe commonalities and differences between the flows of interest and incompressible turbulent boundary layers, with a view to understanding when and how knowledge from the better-studied incompressible case may be applied to compressible turbulence, as well as characterizing the physical forcing exciting truly compressible responses in the flow. We exploit the latter for a proof of concept demonstration of modeling the disturbance field radiated into the freestream from a turbulent boundary layer, an important concern for stability experiments on models mounted in the freestream.

FINAL REPORT

Contract/Grant Title: Influence of Mach number, non-adiabatic walls and nonlinear interactions in resolvent analysis of compressible turbulent boundary layers

Contract/Grant #: FA9550-20-1-0173

Reporting Period: June 2020 to June 2023

Abstract

The challenges associated with observing high-speed boundary layers are well known. In the turbulent regime, there is rarely sufficient observation time to fully characterize statistics or structures. Models for understanding and for large eddy simulation typically rely on a range of assumptions and empirical but tested assumptions. In this work, we seek to develop resolvent analysis for developing turbulent boundary layers under conditions approaching realistic for applications of interest, in particular with regards to Mach number and wall cooling. The subsequent results are used to describe commonalities and differences between the flows of interest and incompressible turbulent boundary layers, with a view to understanding when and how knowledge from the better-studied incompressible case may be applied to compressible turbulence, as well as characterizing the physical forcing exciting truly compressible responses in the flow. We exploit the latter for a proof of concept demonstration of modeling the disturbance field radiated into the freestream from a turbulent boundary layer, an important concern for stability experiments on models mounted in the freestream.

Accomplishments

RESEARCH OBJECTIVES

Extend resolvent analysis to study hypersonic Mach number, non-adiabatic wall, spatially-developing compressible boundary layers, and consider the impact of the modifications of the nonlinear forcing due to compressibility and wall boundary condition.

Specific objectives are outlined as follows:

1. Extend the present quasi-parallel resolvent formulation, which is based on the exceedingly cheap computations associated with a one-dimensional turbulent mean profile, to the spatially-developing case, incorporating state-of-the-art techniques to exploit the low-rank nature of the resolvent operators associated with a two-dimensional mean field.

2. Investigate resolvent model representations of such hypersonic turbulent boundary layers, i.e. determine the weights on the linear resolvent modes to optimally reconstruct the flow-field. Objectives 2 and 3 will require accessing new, higher Mach number DNS databases such as the data of Zhang et al (2018), Fu et al (2019) and numerical resources at the Stanford Center for

Turbulent Research and the von Karman Institute (discussion of informal collaboration in this regard is already under way).

3. Extend the previous investigation to incorporate higher Mach numbers, where effects of compressibility identified in our earlier study are expected to dominate essentially incompressible physics.

4. Consider the influence of a non-adiabatic wall boundary condition on the analysis. It is known that the mean velocity for a non-adiabatic wall does not collapse with semi-local scaling, so some deviation from incompressible and adiabatic wall results (which have been shown to collapse well where acoustic modes are not important) are expected in the analysis. Preliminary results (Figure 4, discussed in the following section) show this to be the case, but a detailed study which characterizes the differences and the wavenumber regimes where they occur is required.

5. Investigate both the form of the resolvent forcing modes (available from the linear analysis) and the forcing obtained from nonlinear interaction of resolvent modes (which differs from the incompressible case because of the fluctuations in density and temperature) in order to identify similarities and differences associated with the introduction of the thermodynamic variables, and the importance of acoustic modes in turbulent boundary layers.

6. Construct a low-order model of the compressible TBL, exploiting the developments from each of the other objectives. The fluctuations and stresses derived from self-interaction of modes feed back to the mean fields, providing a means to support the input mean fields, effectively as constraint on nonlinear low-order models.

ACCOMPLISHMENTS DURING REPORTING PERIOD

Work has been completed on objectives 1-5 and for a specific configuration under objective 6. Here we provide a brief summary of activities throughout the award period. More details are given in the Technical Update section. The work has led to the following accomplishments:

- Implementation of local and biglobal resolvent analyses to examine spatially-developing, high-speed turbulent boundary layer flows.
- Characterization of the response of a supersonic flow with an adiabatic wall to stochastic forcing.
- Characterization of the response of supersonic and hypersonic boundary layers with adiabatic walls to deterministic forcing.
- Distillation of the key variations with increasing Mach number and with wall cooling for local resolvent analysis, i.e. under a quasi-static approximation and considering a one-dimensional mean profile and for the biglobal case.
- Identification and verification of the effects of dilatation on compressible wall turbulence.

- Implementation of a Helmholtz decomposition of the **forcing** in the resolvent framework. While other authors have considered this decomposition on DNS fields (the response in our approach), the forcing is shown to have a clean decomposition into effects common with incompressible flows and those associated only with compressible ones.
- Leveraging of the forcing decomposition to model the disturbance field radiating to the freestream and comparison with DNS results. Significant results include the connection between waves radiating from the turbulent boundary layer into the freestream with the inviscid Mack waves that are well known in laminar flow; the isolation of Mach waves via masked resolvent analysis; identification of the source of Mack waves in terms of the forcing exciting them via the equations of motion; connection between the observations of wave angle and resolvent predictions.
- Differentiation between cases where a 2D, biglobal analysis is required from those where the cheaper 1D case suffices. Where do 2D effects become important, and how can they be efficiently modeled within the objectives laid out in the proposal.
- Application of the resolvent methods to modeling radiation from the boundary layer to the freestream, i.e. to connect the freestream disturbance field affecting modeling testing to the tunnel wall boundary layer characteristics.

DISSEMINATION

Work pertaining to this grant has been presented annually at the 2021 and 2022 APS Division of Fluid Dynamics Annual Meetings (and the upcoming 2023 Meeting) and the AIAA SciTech 2022 meeting. We anticipate a submission to the 2024 AIAA Aviation meeting pertaining to work under this funding.

Impacts

The major impact of the work under this grant has been to elucidate differences and commonalities between incompressible and compressible wall turbulence, channels and zero pressure gradient boundary layers in particular, and the effects of Mach number and wall cooling on that analysis using resolvent-based techniques. We have exploited self-similarity of the mean profile as a way to understand self-similarity of turbulent response to forcing, and the Helmholtz decomposition to separate forcing mechanisms that are common across Mach number from those specific to supersonic and hypersonic Mach numbers, and the associated physical structures corresponding to the latter.

This novel interpretation of the nonlinear forcing and linear response in wall turbulence has the potential to permit separate modeling of both types of effect, including for the more practical cooled wall cases as well as adiabatic walls. In separate work, we are investigating how to exploit general resolvent findings to improve the fidelity of low-order and computational models in incompressible flows. This work could naturally be extended to the high-speed regime.

A key aspect of the work is the ability to address the modeling of the Mach wave radiation from the boundary layer into the freestream for hypersonic flows, a question with direct implications for experimental test facilities, and which we have been continuing to investigate as the grant concludes.

In terms of personnel, the graduate research assistant (Stroot) primarily working on the grant has passed his thesis candidacy exam and is thus on track to complete a Ph.D. in approximately the next 12 months in the area of low-order modelling of hypersonic, turbulent wall flows. A second graduate student (Gomez) contributing to the research recently successfully defended his Ph.D. thesis and will continue as a postdoctoral fellow at Stanford University, effective November 2023. The postdoctoral scholar (Madhusudanan) who began the work on this project completed a Simons Fellowship at the University of Cambridge and is now a DST-INSPIRE Faculty Fellow at the Indian Institute of Science.

Changes

There are no changes to report.

Technical Updates – Final Report

We augment the description of Accomplishments above with technical details concerning each of the objectives.

1. Resolvent analysis for spatially-developing boundary layers

As in our previous effort related to this grant, we develop resolvent analysis for 1D mean fields (local or 1D analysis), and extend the effort to 2D or biglobal resolvent analysis, which takes specific account of the effects of streamwise development of the boundary layer. Further, we consider masked analyses, in which the response may be restricted to the freestream, i.e. outside of the boundary layer (Figure 1). Full details of the approach may be found in Bae, Dawson & McKeon (2020) and Madhusudanan & McKeon (2022). Notably, we employ the Chu norm for the analysis.

Figure 1: Local and biglobal resolvent analyses, showing masking for the biglobal case in which response is restricted to the freestream.

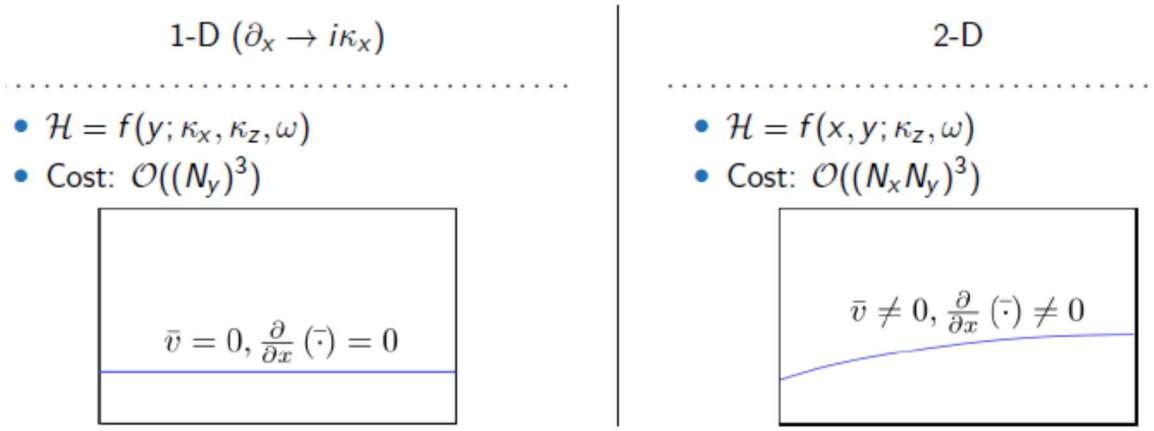

Figure 2: comparison of local and biglobal resolvent analysis domains and costs.

We consider explicitly the cost of the biglobal vs. the local analysis, as shown in Figure 2, in order to determine when the biglobal response may be estimated in terms of the much cheaper, constrained local response.

2. Resolvent response for hypersonic boundary layers (stochastic forcing)

We began work on this grant by considering the stochastically-forced resolvent (which gives insight into the globally most amplified structures by exciting all possible responses). A sample result over a range of Mach number, Ma, for an adiabatic wall laminar boundary layer, where the analytical base profile allowed us to calibrate our approach and the numerics. Figure 3 shows the resolvent norm in the streamwise/spanwise, (k_x,k_z) plane (results are integrated over wavespeed) for Mach numbers in the range 6-10. Forcing is applied to all variables and the footprint of streaks, elongated regions of coherence for low k_x can be seen in all variables across the Ma range. When the forcing is restricted to the velocity components only, i.e. the density and temperature forcing is removed, the appearance of streaks remains. This motivated a more detailed investigation of the action of the forcing terms. Further, the influence of wall cooling was investigated on the resolvent response.

Considering next the deterministic forcing of the resolvent on a mode-by-mode basis, (k_x, k_z, c), where c is the wavespeed, we examined decompositions to isolate the parameter ranges where the response is dominated by velocity vs. density and temperature. The same naïve restriction to velocity forcing did not lead to a separation of the responses (Figure 3, top row), while a very clean separation is obtained by decomposing the forcing into solenoidal and dilatational components given by the singular value decomposition of the resolvent. The separation of the two different responses in (k_z,c) space for a given $k_x$is clearly associated with the relative sonic line, demarked by the dashed black line. For long spanwise wavelengths, the response is isolated to be driven by the dilatational forcing, f_d. Streamwise elongated streaks are dominantly driven by the solenoidal forcing, with an increasingly important response associated with the dilational forcing as Ma increases (Figure 4).

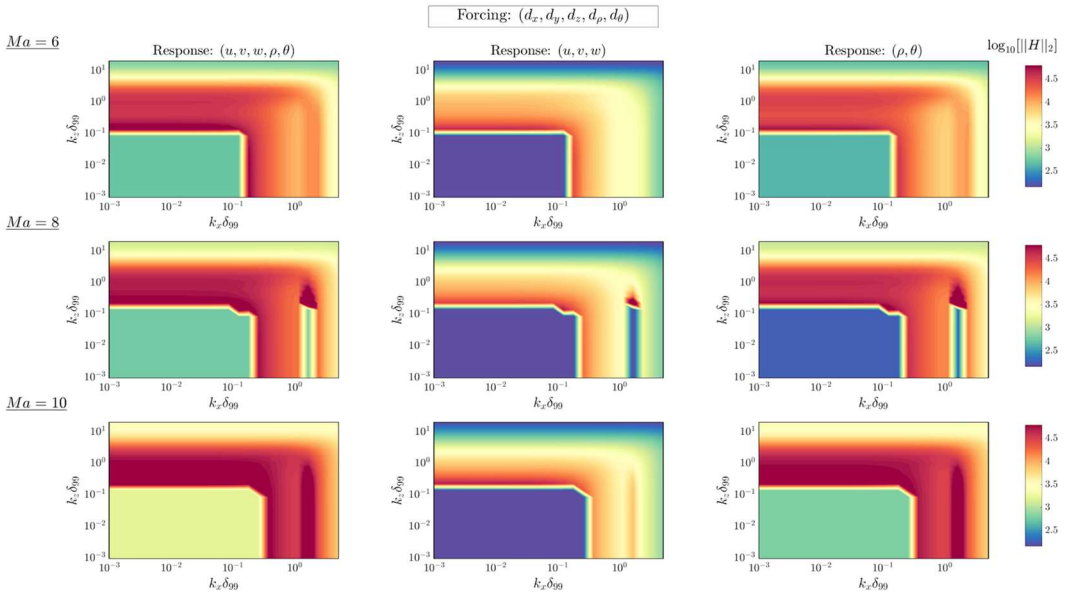

Figure 3: For fixed streamwise wavenumber, Ma=6, Re=300, magnitude of the first singular value of the resolvent. Forcing is applied to all variable and response is separated out into velocity components and density/temperature.

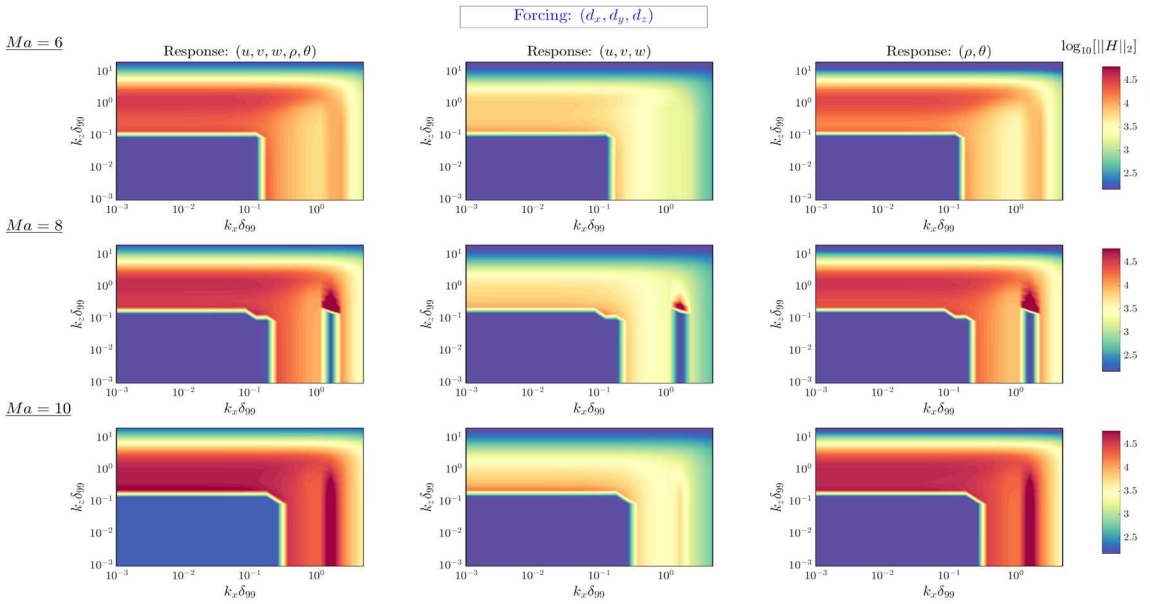

Figure 4: As in Figure 1, but with forcing restricted to the velocity variables only. The footprint of streaks (low streamwise wavenumber) remains in the density and temperature response.

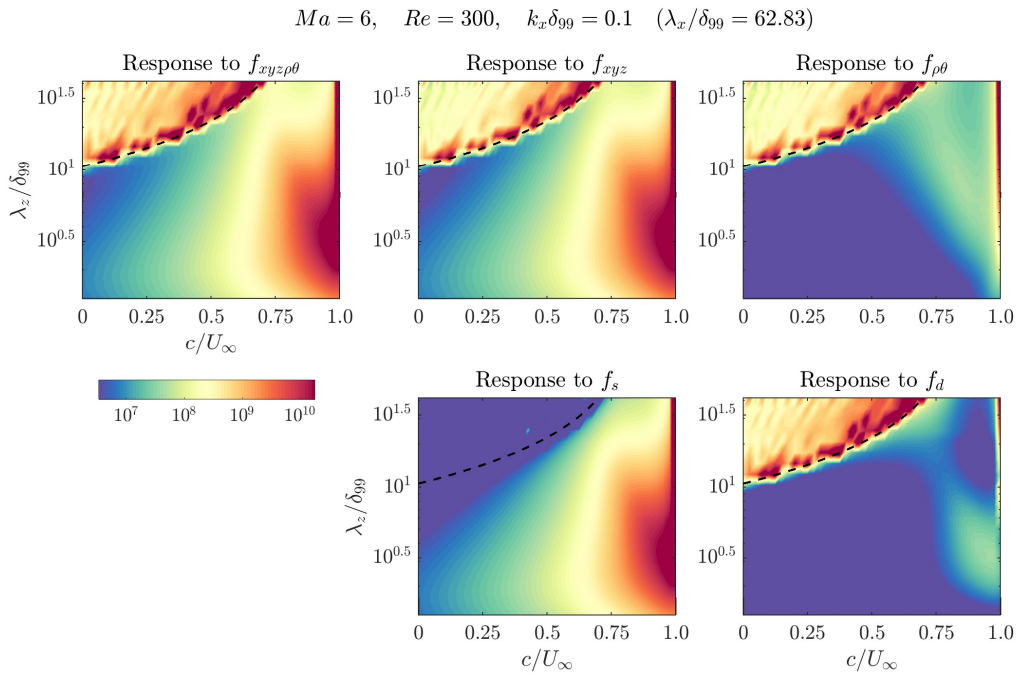

Figure 5: For fixed streamwise wavenumber, Ma=6, Re=300, magnitude of the first singular value of the resolvent for a sweep across spanwise wavenumber and wavespeed. Clockwise, from top left: response to full forcing, response to forcing in the three velocity components only, response to forcing in the density and temperature only, response to dilatational forcing, f_d, and response to solenoidal forcing, f_s

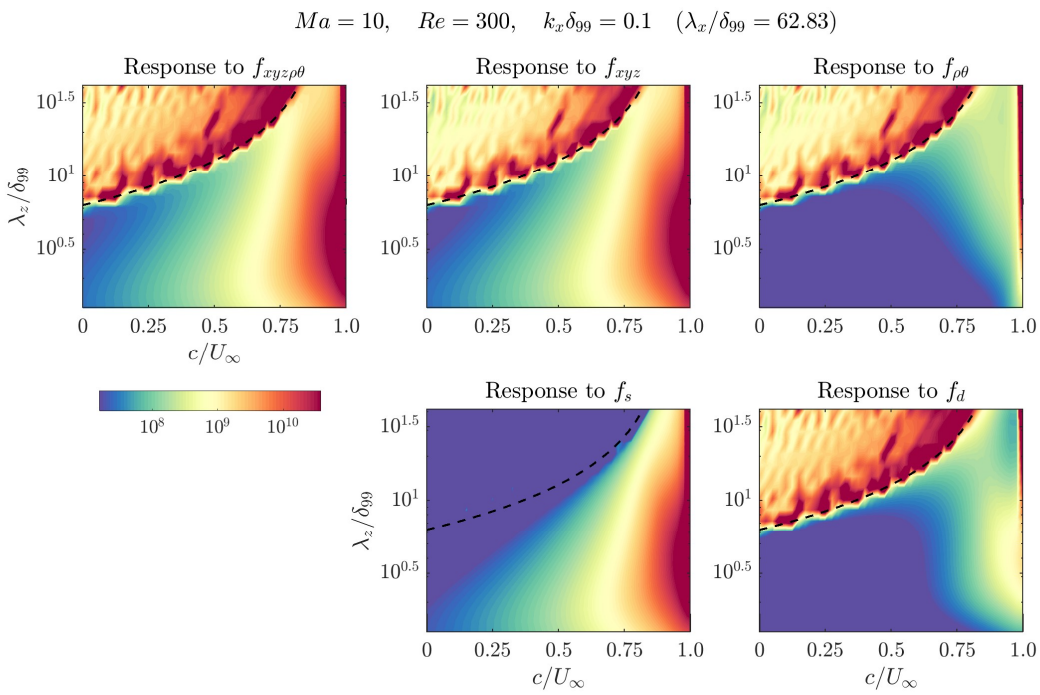

.

Figure 6: As in Figure 5, but for Ma=10.

Finally, Figure 4 shows that the supersonic mode is almost entirely captured when the forcing to the resolvent is solely dilatational. The difference between the red lines and black symbols is due to a small remnant of the effect of solenoidal forcing, which can be predicted from the governing equations. In ongoing work, we are trying to identify the scaling of this effect with Mach number, to assist with modeling of the supersonic modes.

3. Resolvent response for hypersonic boundary layers (deterministic)

The stochastic response gave some indication of the importance of isolating the forcing via the Helmholtz decomposition into solenoidal and dilatational components and the separate treatment of velocity and thermodynamic responses. We moved on to explicitly consider these for the case with deterministic forcing under the quasi-parallel assumption.

The importance of the relative sonic speed, demarking disturbances with wavespeeds that are relatively subsonic from those moving supersonically relative to the freestream, had been identified in our previous work (Bae et al). Under this grant, we showed that the subsonic disturbances can be considered to be identical across Mach range for canonical flow configurations with similar mean profiles, i.e. under a semi-local scaling such as that due to Trettel & Larsson for the compressible case.. Figure 7 shows the integrated response (resolvent norm, σ_1) for M=0 and M=4 cases, with the same gray line identifying an isocontour associated from the M=0 case and the diagonal dashed line the relative sonic condition.

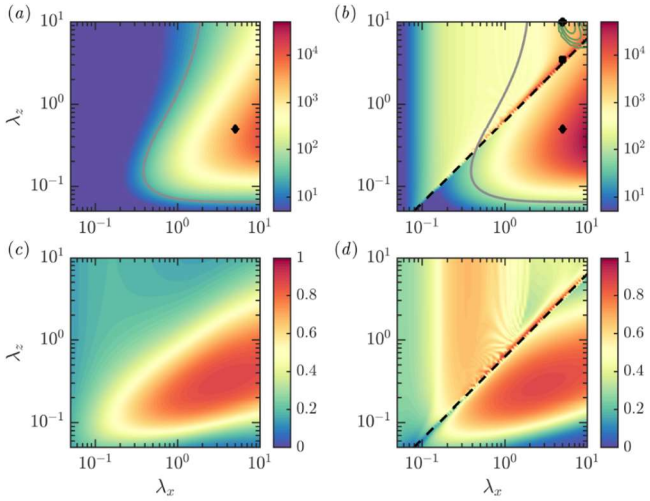

Figure 7: (a,b) The leading resolvent gain σ_1 as well as (c,d) the fraction of energy captured by the leading resolvent mode LR=$\sigma_1^2/(\Sigma_i \sigma_i^2)$, are shown as a function of the streamwise and spanwise wavelengths (lx, lz) and a fixed phase speed c corresponding to $U^+(y^+=15)$. (a,c) An incompressible boundary layer with Re_τ= 450 and (b,d) a compressible boundary layer with Ma=4 and Re_τ = 400 over an adiabatic wall are considered. The black dashed line in (b,d) indicates the relative Mach number equal to unity. The green contours at the top right-hand corner for the compressible case indicates the region of the wavenumber space that is unstable. The grey contour line in (a) indicates 1/3rd of the maximum energy in the incompressible case, and the same contour (computed from the incompressible case) also appears in (b) for comparison. The black symbols indicate the modes that are discussed in later figures.

Figure 8 shows the kinetic energies of the rank-1 approximation of the resolvent, i.e. associated with spatially-integrated ψ_1 for a subsonic mode, including the full response and the separated solenoidal and dilatational components. The separation is relatively clean, however the picture is even clearer when we apply the Helmholtz decomposition to the forcing, ϕ_1 , rather than the response, ψ_1 .

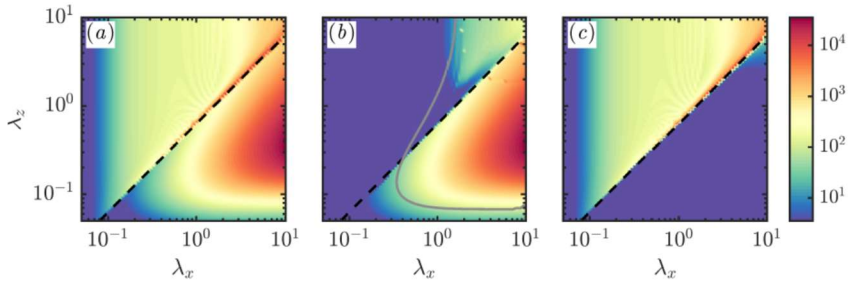

Figure 8: The kinetic energy of (a) the leading resolvent response ψ_1 and of (b) the solenoidal and (c) the dilatational component of the velocity from ψ_1 is shown as a function of the streamwise and spanwise wavelengths and a fixed phase speed c = $U^+(y^+=15)$.

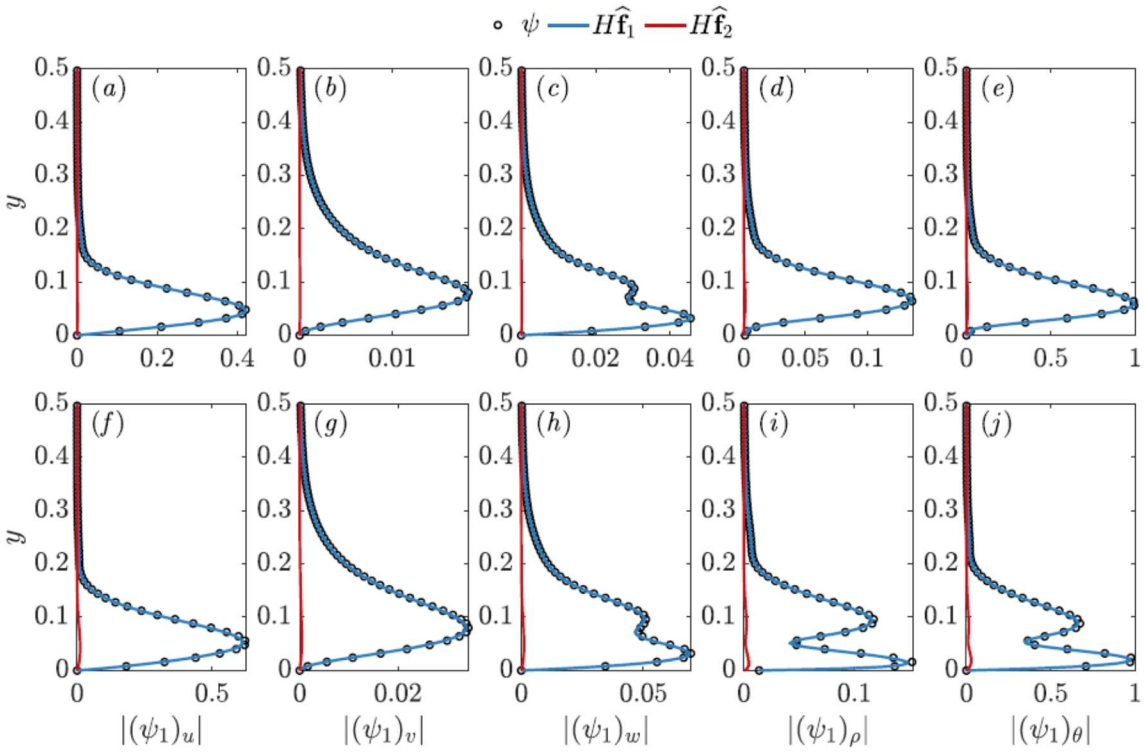

Figure 9: The response of the resolvent operator to the full leading resolvent forcing mode (black) as well as the response to the two components of the forcing: solenoidal (blue) and dilatational (red) are shown. Subsonic modes for two compressible boundary layers are shown: (a-e) Ma=4 and Re_τ = 400 over an adiabatic wall and (f-j) Ma=6, Re_τ=450 with θ_w/θ_{ad}=0.25. The (a,f) streamwise, (b,g) wall-normal and (c,h) spanwise velocities as well as the (d,}) density and (e,j) temperature are shown.

Figure 9 shows that the entirety of the subsonic mode response is captured by the solenoidal part of the forcing (Mach 4 and 6 flows with adiabatic and cooled walls, respectively, shown).

For supersonic modes, we make two observations. First, the response in the freestream is restricted to supersonic modes (not shown), as would be expected. Second, the supersonic modes are forced in the most part by the dilatational forcing, with a small solenoidal part that can be easily identified via the equation governing the pressure fluctuations. An example mode in support of this result is shown in Figure 10.

Importantly for what follows, the freestream region of the pressure, i.e. the radiation to the freestream, is well-described by the well-known inviscid Mack relationship (Figure 11) developed for instability studies, which can be exploited for modeling purposes.

An analytical relationship for the inclination to the wall of the radiating pressure wave can be determined in terms of the aspect ratio and the phase speed of the mode (Figure 12). The range of angles spans those determined to be the statistically dominant ones in DNS of flows under a range of conditions; the actual prediction from the resolvent model depends on the nonlinear forcing induced in the flow.

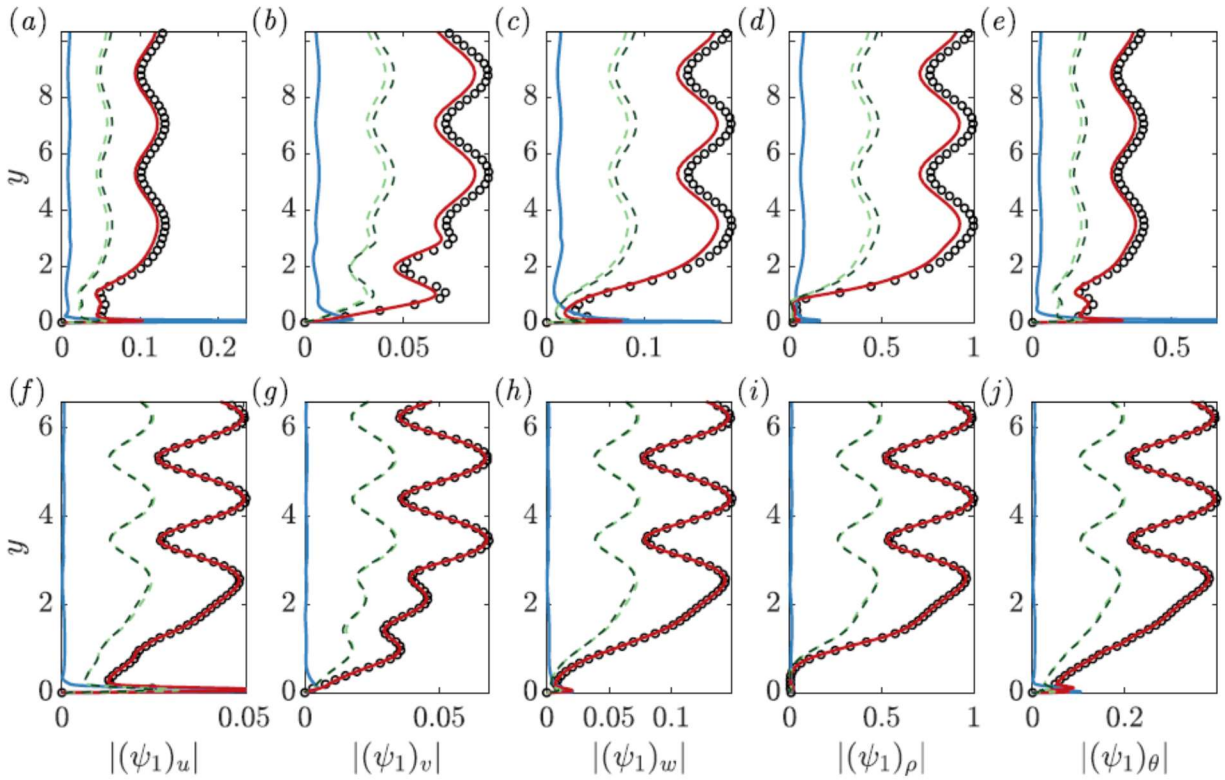

Figure 10: The response of the resolvent operator to the full leading resolvent forcing mode (black) as well as the response to the two components of the forcing: solenoidal (blue) and dilatational (red) are shown. The two green responses are to the thermodynamic and velocity contribution to the dilatational forcing. Supersonic modes that fall close to the relative Mach equal to unity lines are shown for two compressible boundary layers: (a-e) Ma=4 and Re_τ = 400 over an adiabatic wall and (f-j) Ma=6, Re_τ=450 with θ_w/θ_{ad}=0.25. Modes that fall close to the relative Mach equal to unity lines are shown. The (a,f) streamwise, (b,g) wall-normal and (c,h) spanwise velocities as well as the (d,}) density and (e,j) temperature are shown.

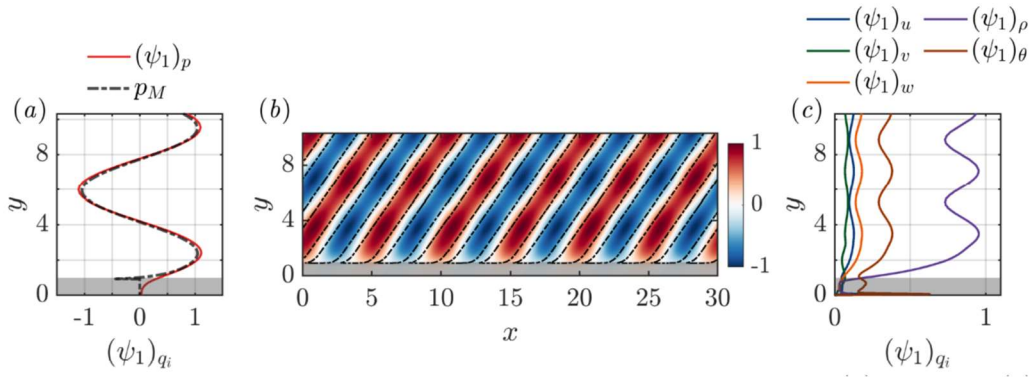

Figure 11: The leading resolvent response for a sample supersonic mode at Ma=4 and Re_τ= 400 over an adiabatic wall. (a) The wall-normal profile of the real part of the pressure from the resolvent mode (red) is compared with the pressure fluctuations from the inviscid Mack wave (black dashed). (b) The pressure fluctuations in a x-y plane is also shown with red (positive) and blue (negative) contours showing the real part of the pressure fluctuation from the resolvent mode and the black contour lines indicating the pressure fluctuations from the inviscid Mach wave at +/- 0.5 of the maximum. (c) The wall-normal profile of the other response components. The grey shaded regions indicate the boundary layer thickness.

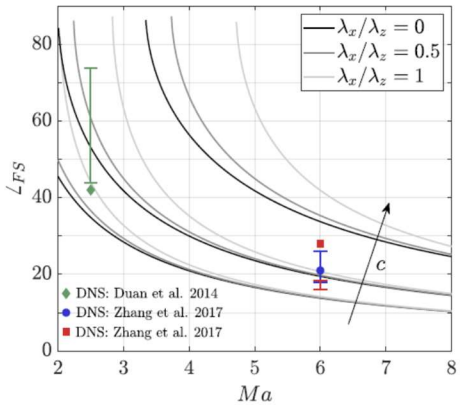

Figure 12: The inclination angle of the radiating Mach waves is shown with respect to Mach number for a range of aspect ratios and phase speeds. Three different phase-speeds of c=0.3,0.5 and 0.7 increasing in the direction of the arrow and three different values of aspect ratios λ_x/λ_z = 0,0.5 and 1.0 are shown. The markers indicate the average inclination angles of the Mach waves from DNS reported in the literature by Duan et al. The DNS data at Ma=6 is for the case of cooled walls, and the two markers indicate two different ratios of θ_w/θ_{ad}=0.76 (blue) and 0.25 (red). The intervals represent the range of inclination angles predicted by the resolvent model under two assumptions: (1) k_y=0 and (2) $U^+(y^+ = 10) < c < U^+(y^+ = 10)$.

4. Towards a low order model of radiated disturbances from hypersonic turbulent boundary layers

In the final piece of the project, we exploited the findings concerning disturbances radiated from the high-speed turbulent boundary layer to make steps towards a computationally efficient and low-order model connecting the freestream statistics to the state of the boundary layer.

First, we explored the relationship between the local and biglobal results for equivalent Reynolds numbers. For the local analysis in a self-similar laminar boundary layer, shown in Figure 13, maximum amplification is associated with a relatively sonic wavespeed and modes normal to the wall, i.e. with inclination angle of 90°.

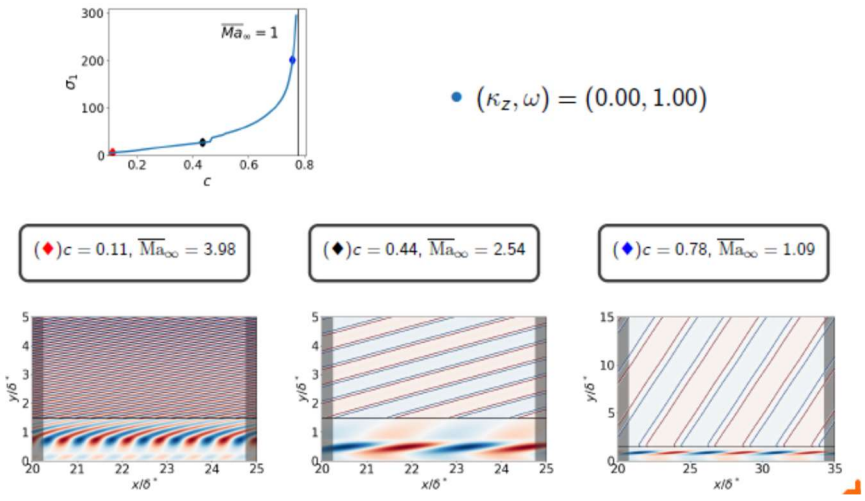

Figure 13: Variation of σ_1 with wavespeed for a given supersonic mode in a turbulent boundary layer. Ma = 4.5 and adiabatic wall. The local resolvent is low-rank; first resolvent modes shown.

The biglobal resolvent for similar parameters is not as low rank, as shown in Figure 14. Here the singular values roll off relatively slowly going down the singular value expansion, with higher modes reflecting beaming (modulation in the streamwise direction). Notably, the maximum amplification occurs for an inclination angle limited by the Mach angle for the flow under consideration.

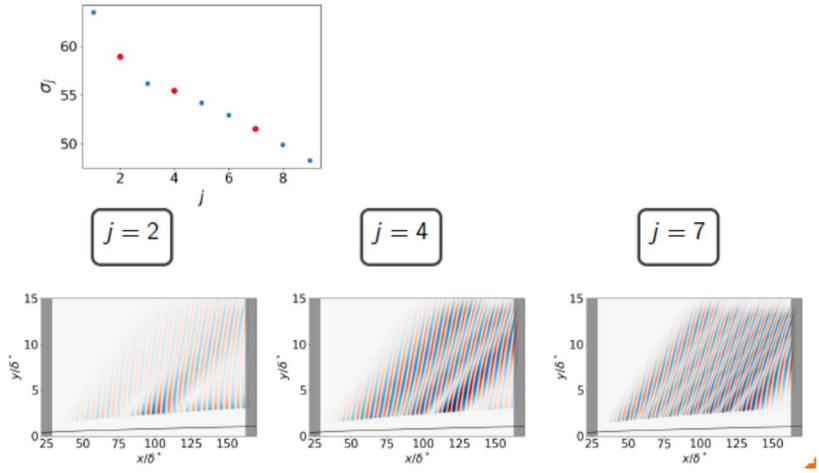

Figure 14: For the same conditions as in Figure 13, but for the biglobal resolvent, radiating structure as a function of position in the singular value decomposition, j.

Nonetheless, the biglobal results can be modeled effectively using local results, the Mach angle restriction and a Gaussian beam envelope (Figure 15).

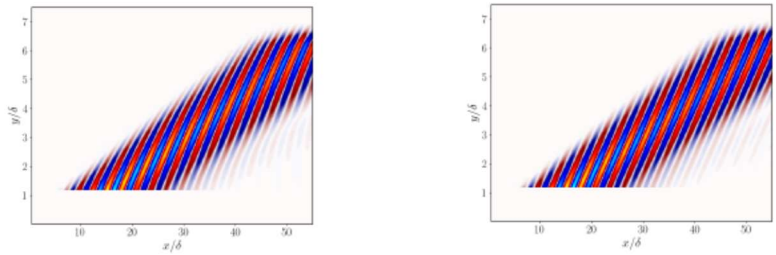

Figure 15: Comparison of the local reconstruction of a given beaming wave (left) and the biglobal results (right) shows reasonable agreement.

Finally, we used local resolvent modes to reconstruct the freestream statistics plotted in Liu et al in their simulation of Ma=8.0 freestream flow above a single wall with a turbulent boundary layer. Just as those authors used a Fourier basis to model the statistics, we used resolvent modes. The origin of these modes can be traced via wavespeed and understanding of relative supersonic mode behavior described above to the region of the boundary layer responsible for the disturbance field. Figure 16 shows the transfer function relationship describing this process and the origin of the disturbances in the buffer layer of the boundary layer, consistent with observations from the DNS of Liu. Inverting this relationship to obtain a predictive model for the freestream disturbance field associated with a given turbulent boundary layer on a tunnel well, is reserved for future work.

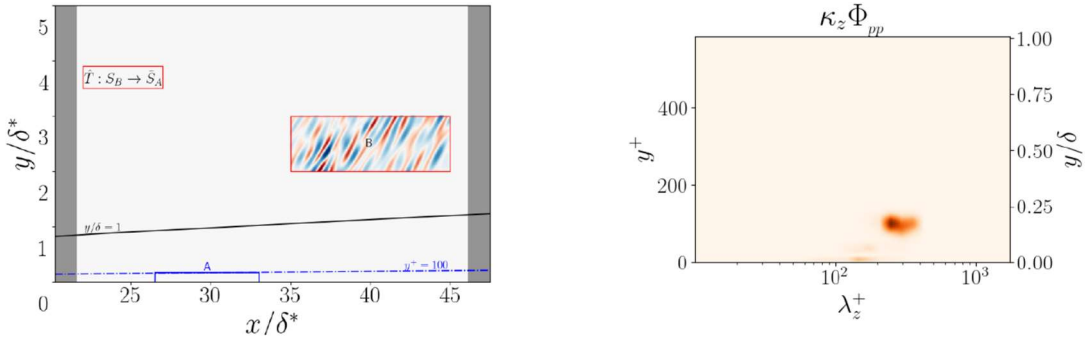

Figure 16: (Left) Schematic showing the transfer function of interest between known freestream disturbance statistics (B) and the state of the boundary layer (A). (Right) spectral representation of the location in the boundary layer of the disturbances that reconstruct the freestream disturbances.

5. Summary

Under this grant, we have performed a fundamental investigation into amplification processes in high speed turbulent boundary layers. By comparison with incompressible wall turbulence at comparable Reynolds numbers, we isolated the Helmholtz decomposition of the nonlinear forcing to the resolvent as an efficient way to separate the driving mechanisms for relatively subsonic and supersonic modes and to provide an effective basis for modeling of the disturbance field radiating to the freestream.

References

Bae, H.J., Dawson, S. & McKeon, B.J. "Resolvent-based study of compressibility effects on supersonic turbulent boundary layers" J. Fluid Mech. 883, A29 (2020).

Chu, B.-T. "On the energy transfer to small disturbances in fluid flow (Part i)". Acta Mech., 1(3), 215.

Duan, L, Beekman, I. & Martin, M. P. "Direct numerical simulation of hypersonic turbulent boundary layers. Part 3: Effect of Mach number." J. Fluid Mech., 672, 245 (2011)

Liu, Y., Schabb, M., Duan, L., Paredes, P. & Choudhari, M. "Interaction of a tunnel-like acoustic disturbance field with a blunt cone boundary layer" https://arc.aiaa.org/doi/abs/10.2514/6.2022-3250 (2022)

Di Renzo, M., Williams, C., Urzay, J. & Pirozzoli, S. "Stagnation enthalpy effect on turbulent compression corner flow at Ma=5" Proc. CTR Summer Program (2022)

Madhusudanan, A. & McKeon, B. J. "A resolvent-based perspective on the generation of Mach wave radiation from compressible boundary layers" (arXiv and under review)

Madhusudanan, M. & **McKeon, B. J.** 'Stochastic forcing to a linearized Navier-Stokes based model for laminar compressible boundary layers' *AIAA-2022-1370.*

Trettel & Larsson, J. "Mean velocity scaling for compressible wall turbulence with heat transfer" Phys. Fluids, 28 (2) 026102 (2016)